Review of Statistical and Analytical Degradation Models for Photovoltaic Modules and Systems as Well as Related Improvements

Sascha Lindig, Ismail Kaaya, Karl-Anders Weiß, David Moser, and Marko Topic

***Abstract*—In this work, we investigate practical approaches of available degradation models and their usage in photovoltaic (PV) modules and systems. On the one hand, degradation prediction of models is described for the calculation of degradation at system level where the degradation mode is unknown and hence the physics cannot be included by the use of analytical models. Several statistical models are thus described and applied for the calculation of the performance loss using as case study two PV systems, installed in Bolzano/Italy. Namely, simple linear regression (SLR), classical seasonal-decomposition, seasonal- and trend-decomposition using Loess (STL), Holt–Winters exponential smoothing and autoregressive integrated moving average (ARIMA) are discussed. The performance loss results show that SLR produces results with highest uncertainties. In comparison, STL and ARIMA perform with the highest accuracy, whereby STL is favored because of its easier implementation. On the other hand, if monitoring data at PV module level are available in controlled conditions, analytical models can be applied. Several analytical models depending on different degradations modes are thus discussed. A comparison study is carried out for models proposed for corrosion. Although the results of the models in question agree in explanation of experimental observations, a big difference in degradation prediction was observed. Finally, a model proposed for potential induced degradation was applied to simulate the degradation of PV systems maximum power in three climatic zones: alpine (Zugspitze, Germany), maritime (Gran Canaria, Spain), and arid (Negev, Israel). As expected, a more severe degradation is predicted for arid climates.**

***Index Terms*—Degradation models, performance loss, photovoltaic (PV) modules, PV systems, service life prediction.**

I. Introduction

BECAUSE of high costs and limited efficiencies, photovoltaic (PV) applications were exclusively used for space applications until the 1970's and 1980's. In the beginning of the 1970's, the dramatic price increase for fossil fuels and an energy uncertainty because of the oil crisis raised the awareness for a need of change in the energy supply [1]. Since then, the interest in renewable energies and solar energy in particular has increased, which in turn led through scientific achievements to a steady reduction in installation costs and performance improvements of terrestrial PV systems. In the late 1990's, the first large-scale PV systems were installed [2]. Nowadays, PV module manufacturers guarantee a performance reduction of no more than 20% within 25 years of operation at standard test conditions (STC) (modules tested indoor under $T_{\mathrm{STC}} = 25\ ^{\circ}\mathrm{C}$, $G_{\mathrm{STC}} = 1000\ \mathrm{W/m^2}$, AM 1.5) and even started to guarantee a maximum degradation of 1%/year for the first ten years. Nevertheless, the actual performance throughout the lifetime is quite uncertain and unpredictable. Laboratory or field determination of PV modules service life under real environmental conditions requires an unacceptable length of time.

PV systems are affected by continuous cycles of temperature, humidity, irradiation, mechanical stress, and soiling. These environmental mechanisms cause different degradation modes to take place within a PV module and reduce the performance of the system. Therefore, it is necessary to develop diagnostic techniques, lower the performance uncertainty, and predict the behavior of PV systems with higher accuracy.

Commonly two approaches, statistical and analytical methods, are used for evaluating degradation rates of PV modules and systems. This report describes quantitative degradation and service lifetime models currently used for PV modules and recommends further improvements. A review of available models and improvements is crucial for accurate life-time calculations of future energy PV systems. The first part of this work focuses on available metrics of variables and the most common statistical models to retrieve the performance loss based on these metrics. The second part deals with analytical models, which pinpoint specific degradation modes and their possible impact on the performance of PV systems.

We believe that a more precise prediction of PV system performance and the capability of linking performance losses to relevant degradation modes will increase public trust in solar energy. Additionally, it will help stakeholders such as investors, PV plant owners, operation and maintenance, and insurance companies as well as other parties involved to favor more beneficial and accurate business models and

Manuscript received June 1, 2018; revised July 27, 2018; accepted September 5, 2018. Date of publication September 26, 2018; date of current version October 26, 2018. This work was supported by the European Union's Horizon 2020 Program under GA. No. 721452—H2020-MSCA-ITN-2016. *(Corresponding author: Sascha Lindig.)*

S. Lindig is with the Institute for Renewable Energy, EURAC Research - Viale Druso 1, 39100 Bolzano, Italy, and also with the Faculty of Engineering, University of Ljubljana, 1000 Ljubljana, Slovenia (e-mail: sascha.lindig@eurac.edu).

I. Kaaya and K. A. Weiß are with the Fraunhofer Institute for Solar Energy Systems, 79110 Freiburg, Germany (e-mail: ismail.kaaya@ise.fraunhofer.de; karl-anders.weiss@ise.fraunhofer.de).

D. Moser is with the Institute for Renewable Energy, EURAC Research - Viale Druso 1, 39100 Bolzano, Italy (e-mail: david.moser@eurac.edu).

M. Topic is with the Faculty of Engineering, University of Ljubljana, 1000 Ljubljana, Slovenia (e-mail: marko.topic@fe.uni-lj.si).

Color versions of one or more of the figures in this paper are available online at http://ieeexplore.ieee.org.

Digital Object Identifier 10.1109/JPHOTOV.2018.2870532

to more efficiently operate and maintain PV systems in the future.

II. PV Modules Degradation Modes

Degradation modes are effects that irreversibly degrade the performance of a PV module/system or may cause safety problems [3]. A great number of different degradation modes are observed in PV modules, both under outdoor operation and indoor testing. The most commonly observed degradation modes include [3]: light induced degradation (LID), solder fatigue failure, silver grid finger delamination, bypass diode failure, delamination, cell cracks, corrosion, polymeric discoloration, ultraviolet (UV) degradation of the cell, polymeric mechanical failure, and potential induced degradation (PID). Each of these degradation modes has different causes and is triggered by different stress factors. Apart from the modes listed, different technical risks, which affect the PV performance and the resulting costs, were found by Moser *et al.* [4]: glass breakage, snail track, defective backsheet, hotspot, soiling, overheating, and failure junction box. An occurring degradation mode can have an increasing impact on the PV performance over time. It develops either in isolation or in combination with other degradation modes or technical risks and might lead to the failure of a PV module. The term failure for electrotechnical devices is defined as "the termination of the ability of an item to perform a required function" [5]. While this definition serves as a clear guideline for most devices, the failure of a PV component is somewhat more complex. For example, although a PV module can still be technically usable, its power output might be too low to verify the continuation of its operation from an economical point of view. Within the scope of this work, a failure is defined as the necessity to replace a PV component, because of its ultimate, economic or safety-related failure. A clear understanding of the definition of a degradation mode is also still a challenge and stress should be put on common nomenclature to define the same degradation mode with the same terminology. For the moment, accelerated aging tests are being utilized in the study of some of these modes. However, there is no proof/evidence that the results from these tests reflect what exactly happens to the modules in outdoor conditions.

III. Degradation Modeling

Degradation models are used to relate a test item's estimated failure time with the wear and tear during its usage period. The failure time is defined as the end of the lifetime of a PV component because of its failure. Degradation models help to quantify the performance loss PV modules and systems are experiencing under operation. Degradation in PV systems is the reduction in efficiency with which a PV system is converting light of the sun into electricity over time [6]. This appears at all levels of a PV system, be it at cell, module or system level. To model PV module degradation modes, the knowledge of internal loads like temperature, chemical conditions, irradiance, and mechanical loads in/on the PV module is required. One very important part is to convert external loads to internal loads of the module.

Models for degradation are generally either data-driven or derived from physical principles via stochastic processes. Although data-driven models are more commonly applied to analyze degradation data, viewing degradation through stochastic processes helps researchers to theoretically characterize the degradation process. Therefore, a coupling of both models could enhance the knowledge of what is happening in PV systems. Data-driven models help to examine the overall performance loss of a system over time and by using analytical models conclusions of what triggered these losses might be derived.

A. Data-Driven Models

Data-driven models are often empirical employed to estimate degradation rates based on statistical analysis of given data sets. The goal of the statistical analysis is to calculate the trend of the PV performance time-series and to translate the slope of the trend to an annual loss rate, in units of %/year [7]. Although these models can provide consistent performance loss rates (PLRs), which are useful for data extrapolation and service life predictions, they do not directly provide evidence for the degradation modes taking place in the module. Other effects such as diffuse soiling, snow, shading or module mismatch have also a direct impact on the performance trend. Therefore, it is more accurate to talk about a PLR rather than a degradation rate.

B. Analytical Models

Analytical models are based on the physical/chemical theories of a specific degradation mode. These models represent the mechanism involved in complex physical/chemical processes. For well-known PV module degradation modes, several analytical models to forecast PV module degradation are available. All these models are based on the principle of understanding the underlying process, but they are still only heuristic models, which do not include the influence of material parameters.

In the following chapters, we discuss the most commonly used performance loss models.

IV. Performance Loss Models

Before applying any statistical model, the observed data are generally treated using filtering techniques depending on factors like irradiance or standard deviation ranges and subsequently averaged or added up over certain time periods. This step is performed as data preparation to minimize outliers and noise and to remove values corresponding to inhomogeneous irradiance conditions on the irradiance sensor and the PV system [8]. Afterwards, a performance metric can be applied to a pretreated data set and the PLR is calculated by using statistical methods. These steps are necessary to minimize seasonal oscillations and to eliminate outliers resulting in the reduction of the overall uncertainty in the estimation of the PLR. In the following, a short overview of the most common performance metrics as well as statistical methods is presented. In Section IV-C, a comparison of the statistical models in question is performed on a case study with data of two PV systems installed at the airport of Bolzano in Italy.

A. Performance Metrics

Statistical performance loss models need to be applied on certain PV system performance-rating parameters. The parameters are expressed through performance metrics, which are measured or calculated in a specified interval. Performance metrics are ideal to compare the performance of different systems in different climates. They can be categorized into three different groups. These are: 1) electrical parameters directly taken from *I–V* curves recorded either outdoor or indoor and corrected to STC, 2) empirical metrics such as PVUSA [9], the 6-k-values performance model (applied in the PVGIS online tool) [10] or the Sandia models [11], and 3) normalized and/or corrected metrics such as performance ratio [7]. Great care has to be taken when selecting performance metrics. The choice as well as possible corrections such as corrected power for temperature and irradiance [12] will influence the results. Therefore, the outcome of a certain performance loss model applied on a specific performance metric needs to be evaluated and put into context to understand the validity of the results.

1) Evaluation of I–V Curves: Electrical parameters of the *I–V* curve include power, voltage, and current at the maximum power point, the open circuit voltage, and the short circuit current. With these parameters, it is possible to calculate the fill factor. A PV systems performance loss is observable when comparing the values of periodically performed measurements of systems in operation [13]. If an unexpected decline in one of the parameters appears, the affected modules can be examined indoors or outdoors, for example, with electroluminescence or thermal imaging cameras. For detailed characterization, indoor measurements can lead to the most accurate results. However, removing PV modules from the field is time consuming with the possibility of damaging the modules during transport and handling. These considerations need to be taken into account to decide which strategy to follow depending on the extent and the complexity of the detected problem and which stakeholders are involved. For example, for insurance claims, outdoor measurement may be sufficient while certified indoor measurements could be required for PV module warranty claims.

2) Empirical Metrics: The empirical metrics presented are models, which aim to obtain performance data while taking into account the dependence between the PV system output and prevailing outdoor conditions [9]. The idea is to receive PV system performance parameter like the efficiency or the maximum power through the application of formulas, which consist of empirical coefficients and weather data. Two widely used models are the 6-k-values performance model and PVUSA. The 6-k-values performance model describes system performance through the relative efficiency η_{REL} correlated to STC as a function of in-plane irradiance G_{POA} and module temperature T_{mod} [14]

$$\eta_{\mathrm{REL}}(G',T') = 1 + k_1 ln(G') + k_2 ln(G')^2 + k_3 T' + k_4 T' ln(G') + k_5 T' ln(G')^2 + k_6 T'^2. \quad (1)$$

Equation (1) has to be fitted to experimental data to obtain the empirical coefficients $k_1 - k_6$. Hereby, the normalized in-plane irradiance $G' = G/G_{\mathrm{STC}}$ and the normalized temperature $T' = T_{\mathrm{mod}} - T_{\mathrm{STC}}$ are considered. An average performance model for each PV type is considered and the k-coefficients are calculated using data from different modules of the same PV technology [10], [14]. This model creates a matrix instead of a single well-defined value for the maximum power point.

Within the PVs for utility scale and applications project, another widely used model, PVUSA, was developed [15], [16]. While calculating corrected power values, it is assumed that the PV system current primarily depends on irradiance and the voltage on module temperature T_{mod}. T_{mod} in turn is strongly dependent on ambient temperature, irradiance, and wind speed. A regression of the systems maximum power output is performed against PVUSA test conditions (PTC) by

$$P_{\mathrm{MPP}} = G_{\mathrm{POA}}(A + BG_{\mathrm{POA}} + CT_{am} + Du_W)$$
$$(G_{\mathrm{PTC}} = 1000\,\mathrm{W/m^2}, T_{\mathrm{PTC}_{AM}} = 20\,^{\circ}\mathrm{C}, u_W = 1\,\mathrm{m/s}). \quad (2)$$

First, measurements at high irradiance values (G $\geq$ 800 W/m^2) in the plane of array (POA) are selected and fitted to calculate monthly values for the coefficients *A*, *B*, *C*, and *D*, applying multivariate regression. Afterwards, the coefficients are used to receive monthly ratings at PTCs (substituting meteorological data values). It should be noted that this methodology is optimized for crystalline silicon PV. An adapted version of the equation including another coefficient *E* was developed to consider thin-film technologies [7], [9].

3) Normalized and Corrected Metrics: Normalized and/or corrected metric parameters are useful when comparing different PV technologies in different climates. Here, PV system performance data are either normalized to comparable, unit-free metrics or corrected in respect to outdoor conditions. One of the most commonly used metrics is the performance ratio (PR), which is an adequate indicator for the quality of a PV installation. The PR is calculated by dividing the final (or array) yield $Y_{f(a)}$ (depending if ac- or dc-power is evaluated) with the reference yield Y_{ref} [17]. The yields are ratios of measured values of power or irradiance with values obtained under STC

$$\mathrm{PR} = \frac{Y_f}{Y_{\mathrm{ref}}} = \frac{P_{\mathrm{AC}}/P_{\mathrm{STC}}}{G_{\mathrm{POA}}/G_{\mathrm{STC}}} \quad (3)$$

$$\mathrm{PR_{DC}} = \frac{Y_a}{Y_{\mathrm{ref}}} = \frac{P_{\mathrm{DC}}/P_{\mathrm{STC}}}{G_{\mathrm{POA}}/G_{\mathrm{STC}}}. \quad (4)$$

When studying the PV performance, it is advisable to use dc-related performance metrics in order to eliminate possible influences because of inverter degradation or misbehavior.

A promising correction method, presented by Belluardo *et al.* [18], evaluates the irradiance and temperature corrected power under STC conditions as follows:

$$P_{T,G\mathrm{corr}} = P_{\mathrm{max}} \frac{G_{\mathrm{STC}}}{G} \frac{1}{1 + \gamma(T_{\mathrm{mod}} - T_{\mathrm{STC}}).} \quad (5)$$

Here, γ is the temperature coefficient of the PV systems power at STC, which is stated on the datasheet. Since γ is retrieved at 1000 W/m^2 and highly temperature dependent, a preliminary data filtering, similar to the filter applied in PVUSA, should be performed to assure the accuracy of the temperature coefficient in use.

Methods, which correct absolute values like power, voltage or current, can be additionally normalized by dividing the corrected value by the nominal installed value under STC. This step simplifies a possible comparison between different PV systems. A clear advantage of these rating techniques is the possibility to evaluate the performance loss in any desired time resolution.

B. Purely Statistical Methods

Statistical analysis methods are used to retrieve trends of performance time-series. These time-series are some sort of performance metrics, which are discussed in Section IV-A. The slope of a trend function can be interpreted as the PLR. It is possible to accumulate these ratings for any given time resolution into an easily comparable annual aging value. The difficulty is to find a good estimation of the PLR since the application of a certain statistical method on a performance metric and a defined filter determines the result significantly. Statistical analysis methods can be divided into model-based methods like linear regression, classical seasonal decomposition (CSD), Holt–Winters (HW) exponential smoothing or autoregressive integrated moving average (ARIMA) and nonmodel-based methods such as seasonal and trend decomposition using Loess (STL). In the following, these commonly used methods are described.

1) Simple Linear Regression (SLR): Performance metrics of any kind are most commonly applied on linear regression because of the straight-forward approach. The fitted trend line is given by

$$\hat{y} = at + b. \tag{6}$$

Hereby, *a* represents the gradient and *b* is the intercept with the *y*-axis. The SLR-algorithm uses the method of least squares. The idea of this method is to sum up squared values of the difference between trend line and actual measurement points and to find the minimum value for this sum. Squares are used to add up only positive numbers and to put more weight on more widely scattered residuals. This method overemphasizes outliers as well as seasonal variations and can result in large uncertainties. Because of that, performance metrics, which reduce seasonal oscillation should be applied if the SLR-algorithm is used.

2) Classical Seasonal Decomposition: Another commonly used statistical model is CSD. By using CSD, the seasonality and a certain irregular component are separated from a set of measured time-series data to receive a clear trend over time. This technique helps to get a fast idea of a performance loss of the system in question. The trend is obtained by applying a centered moving smoothing on a time-series with a certain seasonal period *m*. When using monthly data, the seasonal period is usually set to 12. Here, the first value is computed by averaging over the first 12 months. Due to the 12-month centered moving average, 6 months at the beginning and 6 months at the end of the observation period are not included in the computation. To calculate the seasonality, the trend is subtracted from the measured data and each month throughout the years of surveillance is averaged. What remains at the end is an irregular component [19]. Depending on the stability of the seasonal component, an additive or a multiplicative model is used as shown in the equations below

$$\hat{y} = T_t + S_t + e_t \quad , \quad \hat{y} = T_t \times S_t \times e_t. \tag{7}$$

Here, *T* is the trend, *S* the seasonality, and *e* the remaining part of the data [7].

3) HW Seasonal model: The HW seasonal model contains a forecast equation and three smoothing equations as shown below

$$\hat{y}_{t+1|t} = l_t + b_t + s_{t-S+1} \tag{8}$$

$$l_t = A(y_t - s_{t-S}) + (1 - A)(l_{t-1} + b_{t-1}) \tag{9}$$

$$b_t = B(l_t - l_{t-1}) + (1 - B)b_{t-1} \tag{10}$$

$$s_t = C(y_t - l_{t-1} - b_{t-1}) + (1 - C)s_{t-S}. \tag{11}$$

Here, l_t is the level, b_t the slope, and s_t the seasonal component. *A*, *B*, and *C* are smoothing parameters. If monthly data are evaluated, the period of seasonality, *S*, equals to the value of 12. The HW model is either additive or multiplicative, depending on the seasonal behavior. In case of evaluating a PV systems performance, the additive method should be selected because the seasonal variations are approximately constant throughout the series. The seasonal component is then computed in absolute terms and has a mean of around zero. The level equation (9) is a weighted average between the seasonally adjusted observation $(y_t - s_{t-S})$ and the nonseasonal one-step-ahead forecast $(l_{t-1} + b_{t-1})$. The slope is a weighted average of the level at time *t* minus the level at $t - 1$, and the trend at $t - 1$. The selection of smoothing parameters determines how fast the exponential weights decline over the past observations. The HW method can be especially useful for computing the future behavior of a PV system [7], [20], [21].

4) Autoregressive Integrated Moving Average: ARIMA is a model, which can contain several methods in a multiplicative way and can be described as ARIMA (p, d, q) (P, D, Q). Here, p is the auto-regressive, d the differencing, and q the moving average order as well as P is the seasonal autoregressive, D the seasonal differencing, and Q the seasonal moving average order. Due to the flexibility of the model, seasonal variations, errors, outliers, and level shifts can be addressed in a proper way. ARIMA is applied using the following [7]:

$$\phi(T)\phi_S(T^S) \bigtriangledown^d \bigtriangledown_S^D y_t = \phi(T)\phi_S(T^S)e_t \tag{12}$$

T is the delay operator, $\phi(T) = (1 - \phi_1 T - \cdots - \phi_p T^p)$ is an autoregressive polynomial in *T* of degree *P*, $\phi(T^S)$ is an autoregressive polynomial in T^S of degree P_S, $\phi(T)$ a moving average polynomial in *T* of degree *q*, and $\phi_S(T^S)$ is a moving average polynomial of degree Q_S in T^S. Apart from that, $\bigtriangledown^d = (1 - T)^D$ is a nonseasonal differencing operator and $\bigtriangledown_S^D = (1 - T^S)^d$ is a seasonal differencing operator and grasps nonstationarity in the relevant location in consecutive periods [22].

The stationarity of the time-series determines the optimal ARIMA model; a transformation using differencing to achieve stationarity might be indispensable. Stationarity is described by a constant mean and variance, resulting in a nonexisting trend and the graph seems more like white noise. There are different

ways to difference a time-series, the simplest and most common way being first-order differencing [23]

$$\hat{y} = y_t - y_{t-1}. \tag{13}$$

Here, the differenced value is the change between two consecutive values of the original time-series. The resulting time-series has T-1 values. Seasonal or second-order differencing are further examples of how to create stationarity within the time-series in question.

The heart of the ARIMA model is the application of autoregression. To perform an autoregression, the desired variable is computed by applying a linear combination of past values of the variable. The general form of an autoregressive model of order p is

$$\hat{y} = c + \phi_1 y_{t-1} + \phi_2 y_{t-2} + \cdots + \phi_p y_{t-p} + e_t \tag{14}$$

where c is a constant and e_t is the remainder.

The moving average model used within ARIMA has a different purpose than the one for CSD. Here, the moving average uses past forecast errors in a model similar to a regression. The aim of the moving average model is to predict a forecast instead of smoothing the trend cycle of past values [21].

While using the software environment R, the function seas, a function within the R-package "seasonal" which automatically performs seasonal adjustments, automatically calculates the optimal ARIMA (p, d, q)(P, D, Q) variables to apply on the data set [24]. For the application of ARIMA within Section IV-C, the extracted parameters for both systems are (0, 1, 1) (0, 1, 1).

5) Seasonal–Trend Decomposition Using LOESS: STL is a continuation of CSD and Loess is a method to estimate nonlinear relationships. The centered moving average is replaced by a locally weighted regression to extract the trend [25]. Because of that, the estimates become more robust and are less affected by missing data and outliers. Similar to CSD, STL decomposes a seasonal time-series into three components (trend, seasonal, remainder) and is described by

$$Y_t = T_t + S_t + R_t. \tag{15}$$

STL contains an inner and an outer loop. Every time a run within the inner loop is performed, the seasonal and trend components are updated. The number of runs within the inner loop are mostly equal to 1 or 2. The outer loop includes an inner loop followed by a calculation of robustness weights. This calculation serves as an input for the following inner loop to decrease the impact of transient, abnormal behavior on the trend and seasonal parts [26].

To better grasp the idea of Loess, the method is explained when applied within the software R. Here, two parameters have to be chosen, the trend window and the seasonal window. The seasonal window is either periodic or the span of the Loess window for seasonal extraction. The smaller the values, the faster the trend and seasonal components can change. A high value for the seasonal window forces the seasonal part to be periodic, in this case just the means for the monthly values are used (seasonal component for January is mean of all January values). After calculating the seasonally adjusted data, (measured data minus seasonality) the trend is Loess-smoothened. This is done by applying local regression on a data window with a certain width. The regression curve is fitted to the data within the window. The closer the points are to the center of the window (higher weight), the greater is the impact on the regression line calculation. The weight is reduced on those points that are furthest from the regression curve. The whole step of regression and weighting is repeated several times to receive a point on the Loess-curve, which is at the center of the window. By moving the window across the data, the complete Loess curve is computed. What follows is that each point of the Loess curve is the intersect of a regression curve and the center of the respective window.

C. Comparison of Statistical Models

The statistical models presented are applied on the uncorrected performance ratio data sets of a mono-crystalline (mc-Si) and an amorphous silicon (a-Si) system using the software R. The mc-Si system contains 14 PV modules and has a rated power of 1960 Watt-peak (Wp). The second installation includes 12 amorphous silicon modules with a power of 1200 Wp. The observed data have a resolution of 15 min and were averaged over whole months. The systems in question were installed in Bolzano/Italy in August 2010 and are evaluated for seven years from March 2011 until February 2018 in order to eliminate initial degradation effects such as the Staebler–Wronski effect or short-term LID. The monitored data are prefiltered to exclude data with performance ratio values below 1% and above 200% and a POA irradiation of less than 50 W/m^2 and more than 1500 W/m^2. This was done to remove extreme outliers and measurement errors. The simplicity of the filter was chosen to intensify possible deviations among the models. The irradiance data are recorded with a pyranometer. For each model, the relative annual PLRs, the corresponding uncertainty and the intercept with the y-axis are given. The PLR of the more sophisticated models are calculated by applying a linear regression to the respective trend, which was extracted through the statistical model. To receive the yearly relative PLR and the corresponding uncertainty, the following formulas are used [27]:

$$\text{PLR} = \frac{12a}{b} \tag{16}$$

$$u_{\text{PLR}} = \sqrt{\left(\left(\frac{12}{b}\right)^2 \times u_a^2 + \left(\frac{-12a}{b^2}\right)^2 \times u_b^2\right)} \tag{17}$$

where a and b are the fitting coefficients of the linear regression, $u_{a,b}^2$ the variances of these fitting coefficients, and u_{PLR} the standard deviation of the PLR. This uncertainty calculation corresponds to a confidence interval of 68%.

Two definitions of the PLR can be found in the literature, in relative terms as PLR $= 12a/b$ or absolute with PLR $= 12a$ [18]. Here, the relative PLR was chosen because it makes it easier to generalize the findings to the energy yield of the array using the initial yield of the plant. The results of these calculations are less aimed to deliver the best possible combination of filtering techniques, performance metrics, and statistical models but are intended to provide a direct comparison between the presented analysis methods. While the uncertainties of the resulting PLRs

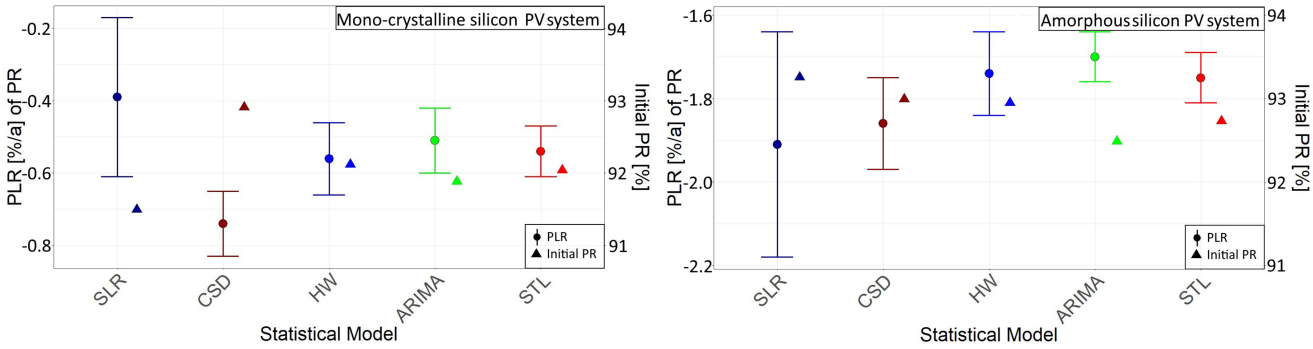

Fig. 1. Comparison of statistical models on PR-data, circles represent PLR including uncertainties (primary axis), triangles represent initial PR (secondary axis), on the left is mc-Si system, on the right is a-Si system.

TABLE I
COMPARISON OF STATISTICAL MODELS

Characteristic	SLR	CSD	HW	ARIMA	STL
Different technologies	PLR with highest uncertainty	Not well suited	Not that well suited	PLR with high accuracy	PLR with high accuracy
Filtering, outlier handling	Crucial, outlier have big impact	Crucial, outlier have big impact	Robust through weighted average	Robust through models flexibility	Robust through locally weighted regression
Time period	Longer time-series better suited	Removing of first & last observations	Shorter time series can be evaluated	Shorter time series can be evaluated	shorter time series can be evaluated
Seasonality	Sensitive to seasonality	Sensitive to seasonality	Insensitive to seasonality	Insensitive to seasonality	Insensitive to seasonality
Stationarity of time-series	Not necessary	Not necessary	Not necessary	Stationarity necessary	Not necessary

were used to rate the statistical models, the remainder, where applicable, serves as a validation of the parameter fit. The remainder should have Gaussian white noise properties, such as being uncorrelated and normally distributed.

In Fig. 1, the relative PLRs, uncertainties and initial PR values are given. The initial value is the intercept with the *y*-axis. The stated uncertainty is the uncertainty of the PLR against the extracted trends, computed by the individual statistical methods.

It can be seen that the performance of the mc-Si system degrades 0.5%–0.6% per year, the one of a-Si close to 1.8% per year. Because of cabling and other system losses the initial PR value is below the theoretical value under STC. As expected, linear regression shows in both cases the highest uncertainty. For all other cases, a trend was first filtered from the data set on which a linear regression was performed. This step leads to an outcome with higher certainties. While all more advanced methods show similar results with regards to the uncertainty of the mc-Si system, STL and ARIMA outperform the others when applied to the a-Si system.

In case of CSD, the loss ratio is for both systems higher in comparison and probably overestimated. In Section IV-B2, it was mentioned that, when using CSD, the first and last months of the data set are lost due to the applied centered moving average. This is visible in Fig. 2. Here, the extracted trend-lines of the PR of the mc-Si system using CSD and STL are shown. Within the first six months of observation, the trend of the PR has a roughly stable value. When applying CSD, this time period is not taken

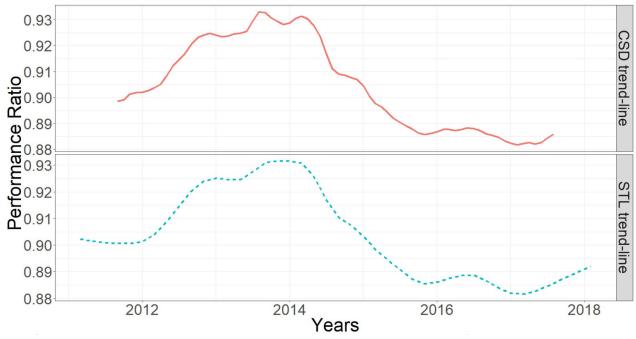

Fig. 2. Trend-lines of CSD- (red-straight) and STL-model (blue-dotted) of unfiltered monthly PR-data of a mc-Si system.

into account and because of this, the decrease is stronger over time. This in turn results additionally in an overestimation of the initial PR value.

Table I summarizes the models in respect to different characteristics of time-series. In general, SLR might serve as a first indication of a PLR determination but is not suited for accurate calculations due to its simplistic approach. It has been shown that the more sophisticated selected analysis methods perform very similar for crystalline systems, both in the estimation of the initial PR and the PLR. An exception hereby is the usage of CSD for short time-series. The exclusion of the first and last observations can falsify the final PLR. When a thin-film system

is subject of the calculations, STL and ARIMA show the best results.

When applying HW, ARIMA or STL, it is very important to perform crucial modeling steps with great care to receive the optimal results. In case of ARIMA, the time-series has to be transformed in order to reach stationarity. Since PV time-series are highly seasonal, a seasonal differentiation is essential. For the same reason, the seasonal window parameter within STL has to be set as periodic and the additive method is preferred when using the HW model.

Filtering is an integral part when computing PLR values. If performance metrics are corrected using temperature coefficients, which are retrieved at a POA irradiance of 1000 W/m^2, an appropriate POA irradiance should be selected. Within this work, the preliminary filter are treating outliers and values corresponding to measurement errors not sufficiently. This was done on purpose to amplify the impact of outliers and measurement inaccuracies on the final results. SLR and CSD treat all values with similar weights and are therefore strongly affected by outliers. HW's weighted average, STL's locally weighted regression, and the combination of similar techniques within ARIMA are well suited for outlier handling.

Another statistical method worth mentioning is the year-on-year model developed by Sunpower [28] and later improved by NREL [29]. It is implemented within the Python RdTools for the analysis of PV data. This method has a complete different approach as the here discussed models, as it is using a loss rate distribution instead of one single value. The gradient between two related data points in consecutive years (hour, day, week, month) determine a single PLR. The median of this gradient, the gradients of all remaining data points of that two years, and all following years determine the final performance loss per year. The power loss rates are computed using a 100% performance baseline value. This approach is excluded within this study. A comparison is difficult to perform because the initial value is preset and, in contrast with the performed computations, the data aggregation is done in an irradiance-weighted manner. Nevertheless, this approach is of special interest if high quality field irradiance data are not available because it can compute the PR based on a modeled clear-sky irradiance.

V. Modeling Specific Degradation Modes Using Analytical Models

In order to explain experimental observations of different degradation modes, analytical models are developed based on the physical/chemical theories of the degradation mode in question. These models are environmental stress oriented. The hypotheses of a particular degradation mode are built depending on specific environmental stresses applied, and on the assumption that the kinetics of a specific degradation mode are influenced by one dominating process. Electrical parameters such as power at maximum power point (P_{max}), short circuit current (I_{SC}), shunt (R_{sh}), and series resistance (R_s) are commonly modeled as degradation indicators. Hence, the environmental stresses and their interactions with the PV module components are assessed based on the reduction of the initial electrical parameter at time ($t = 0$) before aging and at time ($t = t$) after aging or in the field.

A. Degradation Models for Corrosion

Corrosion is one of the most occurring degradation modes in PV modules [30]. Corrosion is caused by the presence of high temperature and high humidity in the module. Humidity can enter the module through the backsheet or the layers of the encapsulant and spread into the module [31], weakening the adhesive bonds between the interfaces. One hypothesis is that humidity, which catalyzes corrosive processes, leads to a formation of acetic acid through the hydrolysis of vinyl-acetate monomers present in the EVA [32]–[34]. Corrosion attacks the metallic connections of PV cells and results in a loss of adhesive strength between the cells and the metallic frame, as well as an increased leakage current and therefore a loss in performance [32]. Empirical models based on power at maximum power point and series resistance as degradation indicators have been proposed to model corrosion according to [35]–[37]. The models are as follows.

1) The Model of Pan [35]

$$\frac{P_{\text{max}}}{P_{\text{max}(0)}} = \exp(-R_D t^{\beta}). \tag{18}$$

2) P_{max} and R_s Models According to Braisaz [36]

$$P_{\text{max}} = \frac{1 - \exp(-B)}{1 + \exp(R_D t - B)} \tag{19}$$

$$R_s = R_{s(0)} + \exp(R_D t - B) \tag{20}$$

where P_{max} and R_s are the output power and series resistance at time (t), $P_{\text{max}(0)}$ and $R_{s(0)}$ are the power output and series resistance at time ($t = 0$), β is the experimental parameter, B is a coefficient to be defined, and R_D is the degradation rate determined according to (21), (22), and (23).

1) Models for Degradation Rate (R_D) Calculation: Kinetic models are developed on the primary assumption that the rate of degradation is proportional to the concentration of water in PV modules and that the rate constant has a Arrhenius temperature dependence. Three models according to [19] and [38] are proposed, namely the Peck's model, the Eyring model, and the exponential model.

Peck's model:

$$R_{D\,.\text{Peck}} = A \exp\left(-\frac{E_a}{k_B T}\right) RH^n. \tag{21}$$

Eyring model:

$$R_{D\,.\text{Eyring}} = A \exp\left(\frac{-E_a}{k_B T} - \frac{b}{RH}\right). \tag{22}$$

Exponential model:

$$R_{D\,.\text{Exp}} = A \exp\left(\frac{-E_a}{k_B T}\right). \exp(m \times RH). \tag{23}$$

Here, E_a is the activation energy of the degradation process [eV], T the module temperature [K], k_B is the Boltzmann constant (8.62×10^{-5} eV/K), and RH is the relative humidity [%].

TABLE II
COMPARISON OF MODELS FOR DEGRADATION RATE

Module 1				
Degradation model	A	E_a [eV]	n,b & m	% deviation
Peck	0.022	0.86	2.17	0.35%
Eyring	0.07	0.71	13.5	1.4%
Exponential	0.012	0.88	0.12	0.5%
Module 2				
Degradation model	A	E_a [eV]	n,b & m	% deviation
Peck	0.12	0.79	2.05	0.41%
Eyring	0.129	0.62	23.0	2.0%
Exponential	0.006	0.81	0.12	0.6%

A, n, b, and m are model parameters. R_D [%/h] is the inverse of the mean time to failure at a given condition. In order to obtain A, E_a, n, b, and m in (21), (22), and (23), the equations can be fitted to experimental data or represented on a logarithmic scale by a straight line, using the following equations:

$$ln(R_{D.\text{Peck}}) = ln(A) - \left(\frac{E_a}{k_B T}\right) + n \times ln(RH) \quad (24)$$

$$ln(R_{D.\text{Eyring}}) = ln(A) - \left(\frac{E_a}{k_B T}\right) - \frac{b}{RH} \quad (25)$$

$$ln(R_{D.\text{Exp}}) = ln(A) - \left(\frac{E_a}{k_B T}\right) + m \times RH. \quad (26)$$

A plot of $ln(R_D)$ versus $1/T[K]$ gives an Arrhenius plot with a slope E_a/k_B and an intercept $ln(A)$.

2) Comparison of Corrosion Models: The models of Peck, Eyring, and exponential were applied to fit indoor data sets (damp heat at 85C/85% RH), of two c-Si modules, with module 1 showing a good performance stability compared with module 2. The models were compared based on the extracted parameters (see Table II) as well as the deviation from the fitted data points. All models are consistent concerning the influence of the activation energy on the degradation rate and that the predicted values are in the range of literature values for polymeric materials, which usually range between 0.6 and 2.0 eV [39]. Nevertheless, the Eyring model shows a significant difference in the extracted activation energy in comparison to that of Pecks and the exponential model. It also has the highest percentage deviation of fitted data points in both cases. Therefore, from this study, we can conclude that the Peck's model has a better fit compared with the other models.

Degradation models are utilized for the simulation of power output degradation for module 1 to predict its performance in three climatic zones: alpine (Zugspitze, Germany), maritime (Gran Canaria, Spain), and arid (Negev, Israel), assuming the degradation is because of corrosion according to Pan and Braisaz. The module temperature is given for a standard c-Si PV module type glass-backsheet construction installed at the three test sites and relative humidity was calculated from ambient conditions according to [40]. For all the simulations, annual mean values of temperature and relative humidity were used. In both cases, the Peck's model was used for degradation rate calculation and both models were fitted to indoor data to extract the model parameters.

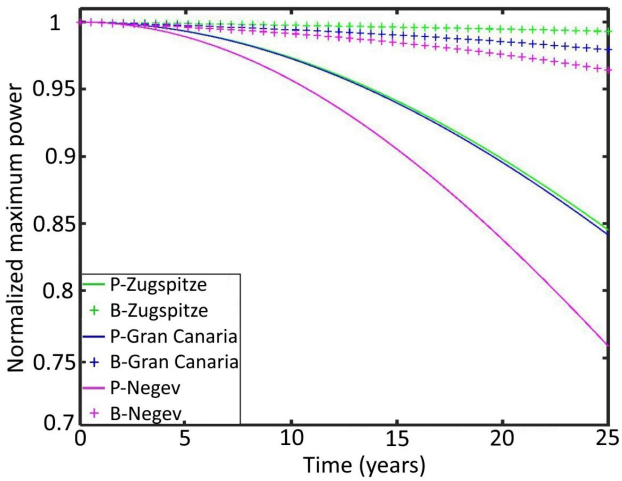

Fig. 3. Module 1. Maximum power degradation models of Pan (P) and Braisaz (B), simulated for three climates: Zugspitze (green), Gran Canaria (blue), and Negev (purple).

Both models show that temperature is the most relevant factor that influences the PV degradation process, visible by the power losses depicted in Fig. 3. This can be seen by a small loss through lower degradation in power for the module installed at Zugspitze, where the climate is characterized by low temperatures and high levels of relative humidity. However, the models completely differ in degradation predictions. According to the simulations, the model of Pan converges at a relatively fast rate compared with the one of Braisaz. This could be due to the influence of the model coefficients such as B and β. Moreover, the time parameter for the Pan model follows a power law, hence β might be an accelerating factor.

B. Degradation Models for PID

PID has been observed in all PV technologies and in almost all operating climates. It does not occur so frequently, but if it does, its effect can lead to a severe performance loss within a short period [4], [41]–[44]. In general terms, PID is caused by the difference in potential between the cells and the support structure of the module. This difference drives a leakage current that can lead to power degradation. Different types of PID occur depending on the module technology. For crystalline silicon PV, two degradation modes can be identified, PID-p (for polarization or passivation) and PID-s (for shunting). PID-p is a temporary and reversible degradation of the passivation layer, which reduces the performance due to a surface recombination increase [45]–[47]. PID-s is because of a leakage current involving an ionic flow of Na+ from the glass, encapsulant or cell surface into the cell, diffusing into the silicon stacking faults and shunting the cell [48]. The sodium incorporation in the Si surface degrades primarily the FF, the V_{oc}, and finally the I_{sc}. The relevant stress factors for PID-s include [42]; high temperature,

TABLE III
PIDHACKE MODEL

A	E_a [eV]	n
4.61	0.99	2.99

relative humidity, system voltage, light, bias-junction potential, and injected carriers. The models proposed for PID degradation according to [36], [43], [44], [49]–[51] are as follows.

1) Pidhacke Model: A parabolic model was proposed by Hacke *et al.* [44] to fit the power degradation of c-Si modules

$$\frac{P_{\max}}{P_{\max(0)}} = 1 - A \exp\left(-\frac{E_a}{k_B T}\right) RH^n \times t^2. \quad (27)$$

The constants A and n are determined by fitting the equation to experimental results. The parameters have to be determined for each module type. This parabolic model is applicable to the beginning of the degradation phases of PID-s, as it can fit the beginning of a sigmoid and does not describe the stabilization phase of the sigmoidal curve. Annigoni *et al.* [49] used the indoor data to determine coefficients of the model for distinct aging contributions (temperature, relative humidity, and time) and then applied the model including a voltage term in (28) to outdoor PID degradation for different climates

$$\frac{P_{\max}}{P_{\max(0)}} = 1 - A \exp\left(-\frac{E_a}{k_B T}\right) RH^n \times t^2 \times U. \quad (28)$$

In this study, a similar approach is adopted to extract the model coefficients in Table III and to simulate maximum power degradation because of PID in three climatic zones; alpine (Zugspitze, Germany), maritime (Gran Canaria, Spain), and arid (Negev, Israel). In all simulations, a constant voltage of 500 V was assumed. The simulation results, shown in Fig. 4, were consistent with the ones of Annigoni, saying that a more severe degradation is predicted for arid climates.

2) Exponential Model: The model was applied by Hacke *et al.* [43] to predict PID occurrence in thin-film modules in the field using accelerated tests. Considering shunting, which is the PID mode that occurs first, an exponential model based on module temperature T and relative humidity RH was found to fit well the PID rate for multiple stress levels of a CdTe module in chamber tests. The power model is of the form

$$\frac{d}{dt}\left(\frac{P_{\max}}{P_{\max(0)}}\right) = 1 - Af(U) \exp\left(-\frac{E_a}{k_B T}\right) RH^n \times t \quad (29)$$

where $f(U)$ expresses the voltage dependency.

3) Model of Hattendorf: The model of Hattendorf *et al.* [50] is based on a matrix of indoor experiments where modules are exposed to varying voltage, module temperature, and ambient humidity. The conditions are varied to determine the model

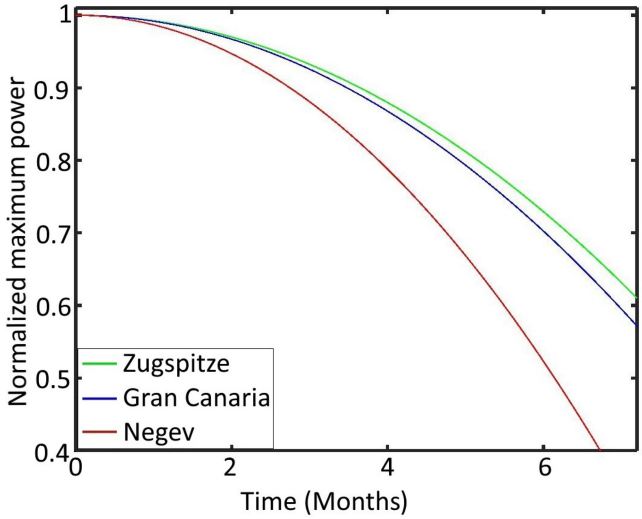

Fig. 4. Simulated normalized maximum power degradation because of PID in three climatic zones; Freiburg (green), Gran Canaria (blue) and Negev (red).

parameters for the module power. The model is written as

$$P_{\max}(U,T,RH,t) = P_{\max(0)}(1 - P(t)) \quad (30)$$

$$P(t) = P_\infty \frac{1 - \exp\left(\frac{t}{\tau_1}\right)}{1 - \exp\left(\frac{t-t_0}{\tau_2}\right)};$$

$$P(U) = \left(1 + \exp\left(\frac{U - U_0}{\Phi}\right)\right)^{-2} \quad (31)$$

$$t_0 = a \times b \times \hat{t_0}; \tau_1(T) = b^2 \times \hat{\tau_1}; \tau_2 = \hat{\tau_2} \quad (32)$$

$$a(H) = \frac{H_0}{H}; b(T) = \exp\left(\frac{T - T_0}{\phi}\right). \quad (33)$$

The model includes six adaptation parameters: $\hat{t_0}$, U_0, $\hat{\tau_1}$, $\hat{\tau_2}$, Φ, and ϕ. H_0 and T_0 are scaling parameters. The function $P(t)$ describes the power loss caused by degradation. $P_\infty(U)$ is its limit for $t \to \infty$, and $a(H)$ and $b(T)$ are the acceleration functions of relative humidity and temperature. For $T = 0$ and $H = 0$, they are equal to 1, therefore $\hat{\tau_1}$, $\hat{\tau_2}$ are the time constants under these conditions. τ_2 remains constant for a given module. To determine the model's parameters, the power degradation is measured as a function of time with the system voltage U as parameters and a fixed humidity H as well as temperature T. The saturating power P_∞ is extracted by fitting $P(t)$ to the measured data.

4) Taubitz Model: Taubitz *et al.* [51] proposed a regeneration model for shunt resistance evolution over time because of PID degradation. The shunt resistance was modeled in three phases: shunting phase, regeneration phase, and transition phase as follows:

Shunting phase:

$$R_{sh}(t) = a_S \exp\left(\frac{-t}{b_S(t)}\right). \quad (34)$$

Regeneration phase:

$$R_{sh}(t) = C_R + a_R \exp\left(\frac{t}{b_R(t)}\right). \tag{35}$$

Transition phase:

$$R_{sh}(t) = a_T(T)(t + b_T(T))^2 + C_T \tag{36}$$

where a_S, b_S, C_T, b_T, $a_T(T)$, $b_S(T)$, $b_T(T)$, C_R, and a_R are constants and have to be determined for a specific module type. Some of them are dependent on the module temperature T. The constants are determined by measuring the times t_S, t_T, and t_R for reaching certain target values.

5) PID Model According to Braisaz et al. [36]: The model is based on shunt resistance R_{sh} degradation as an indicator, as it is the most important parameter for PID. The evolution of R_{sh} as a function of voltage, temperature, and relative humidity was modeled as

$$R_{sh}(t) = \frac{R_{sh(0)}}{1 + aR_D t} \tag{37}$$

$$R_D = A \times U \frac{B}{1 + \exp(-C(RH) + D)} \exp\left(-\frac{E_a}{k_B T}\right) \tag{38}$$

where R_{sh} is the shunt resistance at time (t), $R_{\text{sh}(0)}$ is the initial shunt resistance, A, B, C, and D are model coefficients, U is the applied voltage, and R_D is the degradation rate.

Recommendation: The model contains many coefficients whose usage is not clearly described, such coefficients might affect the physical interpretation of the results when used inappropriately. Therefore, we recommend that one should have a prior knowledge of the impact of the parameters on which the coefficients are being applied to the degradation process in question.

C. Models for UV Degradation

UV light exposure has been reported to cause PV module degradation in a number of ways. Exemplary, it could result in discoloration of the encapsulant material [52] or delamination at the glass encapsulant or cell encapsulant interface [53]. The parameter most impacted by UV exposure is the short circuit current (I_{sc}). Braisaz *et al.* [36] proposed a model for short circuit degradation because of UV exposure over time. They found that the degradation curve is not linear but an exponentially decreasing curve. The short circuit is modeled as a function of UV as

$$I_{sc}(t) = I_{sc(0)} - aD_{\text{UV}}(t) - b(1 - \exp(-CD_{\text{UV}})(t)) \tag{39}$$

$$D_{\text{UV}}(t) = \int_0^t E(u) \times 5.5\% \, \mathrm{d}u. \tag{40}$$

Here, D_{UV} is the UV dose in MJ/m^2 or kWh/m^2, I_{sc} is the short circuit current at time (t), $I_{\text{sc}}(0)$ is the initial short circuit current, and a, b, and C are model coefficients. The multiplication by 5.5% is because the UV radiation (280–400 nm) is approximately 5.5% of the total light spectrum $E(u)$ [54].

1) Schwarzschild Law: The Schwarzschild Law has been applied by Gu *et al.* [55] to study the effect of intensity and wavelength of spectral UV light on discoloration of laminated glass/EVA/PPE PV modules. The law is a function of intensity as

$$k = A(I)^p. \tag{41}$$

Here, k is a constant, I the intensity, and p is the Schwarzschild coefficient.

Recommendation: When applying this expression in performance (power) prediction models where other loads are also applied, the parameter p must be calibrated according to the knowledge of severity ranking [56].

D. Degradation Models for Delamination, Fatigue Solder Failure, and Cell Cracks

1) Coffin–Manson's Equation: The model is used to predict degradation modes caused by temperature cycling such as encapsulant delamination, fatigue solder failure, and cell cracks. According to Escobar and Meeker [38], the model describes the number of cycles to failure as

$$N = \frac{\sigma}{(\Delta T)^{\beta_1}} \tag{42}$$

where ΔT is the temperature range and σ and β_1 are properties of the material and test setup. The cycles-to-failure distribution for temperature cycling can also depend on the cycling rate (e.g., because of heat buildup). An empirical extension of the Coffin–Manson relationship that describes such dependencies is [38]

$$N = \frac{\sigma}{(\Delta T)^{\beta_1}} \frac{1}{(\text{freq})^{\beta_2}} \exp\left(\frac{E_a \times 11605}{T_{\max}(K)}\right) \tag{43}$$

where freq is the cycling frequency and E_a is a quasi-activation energy.

2) Crack Propagation Model: The model was suggested by Braisaz *et al.* [36] and it was applied to simulate the degradation of the short-circuit current I_{sc} due to the expansion of cell cracks caused by temperature. The model takes the form

$$C_a(t) = C_a(t-1) + \frac{1}{x\left(\frac{125}{T_a}\right)^m}. \tag{44}$$

$C_a(t)$ is the crack activation at time (t), $C_a(t-1)$ the crack activation at time $(t-1)$, T_a is the daily temperature amplitude, m a model parameter, and x is the number of thermal cycles. The crack activation/propagation model is dependent on the daily temperature amplitude T_a.

3) Damage Accumulation Model: The model was used by Bosco *et al.* [57] in order to calculate the solder fatigue damage in seven cities investigated in their study and compared with FEM simulated results. They found out that the model fits well to the simulated calculations. The model is written as

$$D = C(\Delta T)^n (r(T))^m \exp\left(-\frac{Q}{k_B T_{\max}}\right). \tag{45}$$

In this equation, ΔT is the mean daily maximum cell temperature change, $T_{\max}$ the mean maximum daily temperature, C a

scaling constant, Q the activation energy, k_B Boltzmann's constant, $r(T)$ the number of times the temperature history increases or decreases across the reversal temperature, T the period of a year, and n and m are model constants similar to those in the Coffin–Manson equation.

4) Backsheet Degradation Model: The model is used to estimate a potential form of the degradation kinetics of the backsheet. This kinetic model was applied by Kempe [58] to model the uncertainty in a 25-year equivalent test for module backside exposure to irradiance and temperatures in different climatic zones. The degradation rate model is written as

$$R_D \approx I^X (b + m \times \text{TOW}) \times (T_f)^{\frac{T-T_0}{10}}. \tag{46}$$

Here, I is the light intensity, X, b, and m are fit parameters, TOW is the time of wetness, T the temperature, T_0 a reference temperature, and T_f is a multiplier for the increase in degradation for a rise in temperature in 10 K steps.

Recommendation: As also mentioned by Kempe, the parameter that describes the effect of time of wetness has very high uncertainties, we recommend careful comparison of the relative change in degradation rate with changes in TOW. In case one wants to extract thermal parameters such as activation energy, the multiplier term (T_f) can be replaced by the Arrhenius term.

E. Model Based on Multiple Stresses

Since degradation of PV modules in outdoor operation is influenced by multiple environmental stresses, models based on multiple stresses are viable for outdoor service lifetime prediction.

1) Model of Gaines: Gaines *et al.* [37] proposed a model for power output degradation based on multiple accelerated environmental stresses. The model suggested is

$$\frac{P_{\max}}{P_{\max(0)}} = [1 - R_D t]^{\frac{1}{\beta}} \tag{47}$$

$$R_D = A f_T f_{RH} f_M f_G f_\omega \tag{48}$$

where R_D is the degradation rate and the factors f_T, f_{RH}, f_M, f_G, and f_ω are associated with a decrease in power output due to effects of temperature T, relative humidity RH, mechanical stresses M (due to temperature differences), gaseous concentration G, and the frequency of the temperature excursion. The mathematical form of each factor is formulated to represent the underlying physical phenomena. An Arrhenius form is used for

$$f_T = \exp\left(-\frac{B}{T}\right). \tag{49}$$

B denotes a constant parameter and T denotes temperature. The effect of relative humidity f_{RH} is represented by

$$f_{\text{RH}} = 1 + (\text{RH})_0 \exp\left(C_0\left(\frac{1}{T_C} - \frac{1}{T_0}\right)\right)^{C-\frac{D}{T}}. \tag{50}$$

The second term in the bracket corrects the relative humidity as a function of temperature, given a specified relative humidity at T_0. C and D are constant parameters. The mechanical/temperature excursion factor f_M is represented by

$$f_M = \left[\frac{\exp\left(G_1\left(\frac{1}{T} - \frac{1}{T_b}\right)\right) + \exp\left(-G_2\left(\frac{1}{T} - \frac{1}{T_b}\right)\right)}{D_0}\right] \times \exp(J\Delta T). \tag{51}$$

The first term in the bracket reflects the stresses arising from differences in expansion coefficients of bonded materials. The constants G_1, G_2, D_0, and T_b are chosen to represent the estimated magnitudes of these fatigue effects. The factor $\exp(J\Delta T)$ estimates the effect of the magnitude of the temperature excursion ΔT, where J is a constant

$$f_G = \left[1 + \frac{G}{G_o}\right]^{E-\frac{F}{T}}. \tag{52}$$

Here, E and F denote constant parameters and T is the temperature. The frequency of the temperature excursion f_ω is represented by

$$f_\omega = \left[1 + \frac{\omega}{\omega_o}\right]^{P-\frac{Q}{T}}. \tag{53}$$

ω is the frequency and P as well as Q are constant parameters. In a constant temperature test, T is a constant and ω is taken to be zero. In the cyclic temperature tests, reciprocal temperature is considered to be a sinusoidal function of time

$$\frac{1}{T}(t) = \tau + \Delta\tau \sin(\omega t) \tag{54}$$

$$\tau = \frac{1}{2}\left[\frac{1}{T_{\min}} - \frac{1}{T_{\max}}\right]. \tag{55}$$

$T_{\min}$ and $T_{\max}$ are the minimum and maximum temperatures associated with the temperature cycles.

Recommendation: The model of Gaines presents the previous approach on multiple stress modeling, however, the user should take caution that this model was developed and applied on PV modules that had a different construction from today's modules. Therefore, its application might need some modification to fit the current PV module construction types.

2) Model of Subramaniyan: Another model to calculate the degradation rate because of combined environmental stresses has been proposed recently by Subramaniyan *et al.* [59]. The model takes into account the effect of both static and cyclic temperature, UV radiation and relative humidity as

$$\text{Rate}(T, \Delta T, \text{UV}, \text{RH}) = \beta_0 \exp\left(-\frac{\beta_1}{k_B T_{\max}}\right) \times (\Delta T_{\text{daily}})^{\beta_2} \times (UV_{\text{daily}})^{\beta_3} \times (RH_{\text{daily}})^{\beta_4} \tag{56}$$

where $\text{Rate}(T, \Delta T, UV, RH)$ is the reaction rate, $T_{\max}$ the daily maximum temperature of the module [K], ΔT_{daily} the daily cyclic temperature of the module [K], UV_{daily} the daily daytime average irradiance [W/m^2], RH_{daily} the daily average relative humidity [%], and k is the Boltzmann constant. The model parameters β_0, which is the frequency factor [s^{-1}], β_1, the activation energy [eV], β_2, the effect of cyclic temperature, β_3, the effect of UV radiation and β_4, the effect of RH, can be estimated from measured data through data fitting techniques. In the scope

of this paper, the model is presented but has not been applied or tested in any way due to a lack of combined stress data. A more detailed description and application of the model can be found in [59].

VI. Discussion and Conclusion

In this paper, several PV system performance loss methodologies are reviewed. Hereby, statistical and analytical models are taken into account.

First, a discussion about statistical models to determine the PLR of PV systems from available outdoor data is presented. The performance loss trend is retrieved by applying filters, performance metrics, and statistical models on data sets. By performing detailed in-depth performance studies, it might be possible to gain a greater understanding about the root causes of the decrease in the power output of PV systems over time. Especially when considering current and voltage behavior, specific degradation modes could be identified and at a later stage verified by visual inspection techniques.

As a first measure, appropriate filtering techniques have to be applied on the data set in question. The choice of the filter will strongly depend on the performance metric and/or statistical model and, in case of an inappropriate filter window, will falsify the final outcome. On the other hand, pretreatment of the data set is necessary to eliminate outliers, noise, and minimize seasonal oscillation. Before deciding which performance metric or statistical model to use, the PV system technology, the length of the observed period, climatic conditions, and mounting system (rack, tracker) should be taken into consideration. Prevailing seasonality, temperature/irradiance dependency of the *I–V* curve parameters and noncorrelated outliers (data errors, shading effects, etc.) will increase the uncertainty of the results and influence the final PLR. The final aim is to receive a clear performance trend. In Section IV-C, the discussed statistical models have been applied on monitored field data of one monocrystalline silicon and one amorphous silicon system to retrieve long-term performance trends. Thereby, the application of SLR resulted in performance ratings with the greatest uncertainties in comparison. The usage of CSD produced performance rates with low uncertainties but due to the elimination of the first and last months of monitored data through the centered moving average, this technique is not recommended for data sets, which just consider short time periods. It was seen that CSD overestimated the performance loss of both systems. The remaining techniques, namely HW exponential smoothing, ARIMA, and STL, are performed on a similar high level of accuracy and the results are almost identical. HW experiences a slightly higher uncertainty when applied to the amorphous silicon PV system. It seems that ARIMA and STL are better suited for noncrystalline PV systems due to their favorable treatment of the temperature behavior of the system in question. These three techniques exclude the seasonal part in time-series of PV performance metrics, which is an important modeling step in order to receive a clear performance trend. Nevertheless, it has to be stressed that the application of statistical models, especially ARIMA, has to be performed with great care and that it is not a rudimentary exercise to retrieve accurate model parameters for more advanced models. In case of ARIMA, the time-series has to be stationary. The model parameters need to be chosen based on the time-series behavior. That means that PV-related parameters, like the varying temperature dependency of different PV technologies, or the prevailing weather conditions have to be taken into account.

Unfortunately, it is not possible to determine if a (or which) degradation mode occurs on the basis of calculated PLRs. Apart from degradation modes, other factors such as shading or soiling might be a reason for a reduced performance. Because of that, it is important to not only study the data of a PV system, but also to undertake regularly visual and electrical inspections and connect the findings with the calculated PLR. An idea of how to isolate the occurrence of degradation modes within a module under surveillance might be the application of the presented models on the short-circuit current, the open-circuit voltage and the fill factor. Hence, it might be possible, together with the inclusion of results from the studies of accelerated tests, to find patterns in the trends of these values.

In the second part of this work, several analytical models for specific degradation modes, which trigger the aforementioned performance losses to a large extent, are further studied. The models proposed for corrosion and PID were implemented to simulate the maximum power degradation in three climatic zones. A strong influence of the climate is evident in all the simulation results where, as expected, a more severe degradation is predicted for arid climates. The key observations in this study are as follows.

1) Although these models give a preliminary approximation of the time-evolution of power performance, they do not provide any information on the physical processes taking place within the module.
2) The models are developed based on numerous assumptions and simplifications, moreover the hypotheses of a particular degradation mode are modeled depending on environmental stress factors and do not take into consideration the influence of material parameters.
3) None of the models is universal, that is, they can well describe the degradation of a specific type of a PV technology and fail on the other. Therefore, it is necessary to be certain that a chosen degradation model is valid for a specific application.
4) The analytical models are developed and validated based on indoor data from accelerated tests. Although some authors went on to simulate outdoor conditions based on indoor observations, a big challenge remains of how to interpret the results for multiple environmental stresses using indoor data.

According to these observations, we recommend further developments for models that take into account both material and multiple environmental stress factors. The development of such models need to be related to indoor as well as outdoor observations.

Acknowledgment

This project has received funding from the European Union's Horizon 2020 research and innovation programme in the frame-

work of the project "SolarTrain" under the Marie Sklodowska-Curie GA No 721452.

REFERENCES

[1] C. S. Solanki, *Solar Photovoltaics - Fundamentals, Technologies and Applications vol. 2*. New Delhi, India: PHI Learning Private Limited, 2012.

[2] I. M. Peters, H. Liu, T. Reindl, and T. Buonassisi, "Global prediction of photovoltaic field performance differences using open-source satellite data," *Joule*, vol. 2, no. 2, pp. 307–322, Feb. 2018.

[3] M. Kontges *et al.*, *Assessment of Photovoltaic Module Failures in the Field*. Report IEA PVPS T13-09:2017, Subtask 3, 2017.

[4] D. Moser *et al.*, "Identification of technical risks in the photovoltaic value chain and quantification of the economic impact," *Prog. Photovolt.: Res. Appl.*, vol. 25, no. 7, pp. 592–604, 2017.

[5] *International Electrotechnical Vocabulary. Chapter 191: Dependability and Quality of Service*, IEC60050-191, International Electrotechnical Comission, Geneva, CH, Standard, 1990.

[6] D. C. Jordan and S. R. Kurtz, "Photovoltaic degradation rates - An analytical Review: Photovoltaic degradation rates," *Prog. Photovolt.: Res. Appl.*, vol. 21, no. 1, pp. 12–29, Jan. 2013.

[7] A. Phinikarides, N. Kindyni, G. Makrides, and G. E. Georghiou, "Review of photovoltaic degradation rate methodologies," *Renew. Sustain. Energy Reviews*, vol. 40, pp. 143–152, Dec. 2014.

[8] D. Moser, M. Pichler, and M. Nikolaeva, "Filtering procedures for reliable outdoor temperature coefficients in different photovoltaic technologies | journal of solar energy engineering | ASME DC," *J. Solar Energy Eng.*, vol. 136, no. 2, pp. 021006-1–021006-10, 2013.

[9] C. M. Whitaker *et al.*, "Application and validation of a new PV performance characterization method," in *Proc. Conf. Record 26th IEEE Photovolt. Spec. Conf.*, Sep. 1997, pp. 1253–1256.

[10] G. H. Yordanov, "Relative efficiency revealed: Equations for k1-k6 of the PVGIS model," in *Proc. IEEE 40th Photovolt. Specialist Conf.*, Jun. 2014, pp. 1393–1398.

[11] D. L. King, J. A. Kratochvil, and W. E. Boyson, "Photovoltaic array performance model," Tech. Rep. SAND2004-3535, 919131, Sandia Nat. Lab., Albuquerque, NM, USA, Aug. 2004.

[12] E. Skoplaki and J. A. Palyvos, "On the temperature dependence of photovoltaic module electrical performance: A review of efficiency/power correlations," *Solar Energy*, vol. 83, no. 5, pp. 614–624, May 2009.

[13] D. C. Jordan, J. H. Wohlgemuth, and S. R. Kurtz, "Technology and climate trends in PV module degradation," in *Proc. 27th EU PVSEC Proc.*, 2012, pp. 3118–3124.

[14] T. Huld *et al.*, "A power-rating model for crystalline silicon PV modules," *Solar Energy Mater. Solar Cells*, vol. 95, no. 12, pp. 3359–3369, Dec. 2011.

[15] C. Jennings, "PV module performance at PG&E," in *Proc. Conf. Rec. 20th IEEE Photovolt. Spec. Conf.*, Sep. 1988, pp. 1225–1229.

[16] C. Whitaker, T. Townsend, and H. Wenger, "Effects of irradiance and other factors on PV temperature coefficients," in *Proc. Conf. Rec. 22nd IEEE Photovolt. Spec. Conf.*, Oct. 1991, pp. 608–613.

[17] *Photovoltaic System Performance Monitoring—Guidelines for Measurement, Data Exchange and Analysis*, IEC61724:1998, International Electrotechnical Comission, Geneva, CH, Standard, 1998.

[18] G. Belluardo *et al.*, "Novel method for the improvement in the evaluation of outdoor performance loss rate in different PV technologies and comparison with two other methods," *Solar Energy*, vol. 117, pp. 139–152, Jul. 2015.

[19] D. C. Jordan and S. R. Kurtz, "Analytical improvements in PV degradation rate determination," in *Proc. 35th IEEE Photovolt. Spec. Conf.*, Jun. 2010, pp. 688–693.

[20] C. C. Holt, "Forecasting seasonals and trends by exponentially weighted moving averages," *Int. J. Forecasting*, vol. 20, no. 1, pp. 5–10, Jan. 2004.

[21] R. J. Hyndman and G. Athanasopoulos, *Forecasting: Principles and Practice*. Melbourne, Australia: OTexts, 2013.

[22] A. Phinikarides, G. Makrides, N. Kindyni, A. Kyprianou, and G. E. Georghiou, "ARIMA modeling of the performance of different photovoltaic technologies," in *Proc. 39th IEEE Photovolt. Spec. Conf.*, Jun. 2013, pp. 0797–0801.

[23] S. G. Makridakis and S. C. Wheelwright, *Forecasting*, 3rd ed. New York, NY, USA: Wiley, Jan. 1998.

[24] C. Sax, *Seasonal: R Interface to X-13-ARIMA-SEATS*, R package version 1.6.1. 2017. [Online]. Available: https://CRAN.R-project.org/package=seasonal

[25] A. Phinikarides, G. Makrides, and G. E. Georghiou, "Comparison of analysis method for the calculation of degradation rates of different photovoltaic technologies," in *Proc. 27th EU PVSEC Proc.*, 2013, pp. 3211–3215.

[26] R. B. Cleveland, W. S. Cleveland, J. E. McRae, and I. Terpenning, "STL: A seasonal-trend decomposition procedure based on loess," *J. Official Statist.*, vol. 6, no. 1, pp. 3–33, 1990.

[27] *Evaluation of Measurement Data—Guide to the Expression of Uncertainty in Measurement,"* International Bureau of Weights and Measures, BIPM-JCGM-100:2008, Sevres, FR, Guide, 2008.

[28] E. Hasselbrink *et al.*, "Validation of the PVLife model using 3 million module-years of live site data," in *Proc. IEEE 39th Photovolt. Spec. Conf.*, Jun. 2013, pp. 0007–0012.

[29] D. C. Jordan, C. Deline, S. R. Kurtz, G. M. Kimball, and M. Anderson, "Robust PV degradation methodology and application," *IEEE J. Photovolt.*, vol. 8, no. 2, pp. 525–531, Mar. 2018.

[30] A. Ndiaye *et al.*, "Degradations of silicon photovoltaic modules: A literature review," *Solar Energy*, vol. 96, pp. 140–151, Oct. 2013.

[31] N. Park, C. Han, and D. Kim, "Effect of moisture condensation on long-term reliability of crystalline silicon photovoltaic modules," *Microelectron. Rel.*, vol. 53, no. 12, pp. 1922–1926, Dec. 2013.

[32] M. D. Kempe *et al.*, "Acetic acid production and glass transition concerns with ethylene-vinyl acetate used in photovoltaic devices," *Solar Energy Mater. Solar Cells*, vol. 91, no. 4, pp. 315–329, Feb. 2007.

[33] K. Whitfield, A. Salomon, S. Yang, and I. Suez, "Damp heat versus field reliability for crystalline silicon," in *Proc. 38th IEEE Photovolt. Spec. Conf.*, Jun. 2012, pp. 1864–1870.

[34] A. Masuda, N. Uchiyama, and Y. Hara, "Degradation by acetic acid for crystalline Si photovoltaic modules," *Jpn. J. Appl. Phys.*, vol. 54, no. 4S, pp. 04DR04-1–04DR04-6, Mar. 2015.

[35] R. Pan, J. Kuitche, and G. Tamizhmani, "Degradation analysis of solar photovoltaic modules: Influence of environmental factor," in *Proc. Annu. Rel. Maintainability Symp.*, Jan. 2011, pp. 1–5.

[36] B. Braisaz, C. Duchayne, M. Van Iseghem, and K. Radouane, "PV aging model applied to several meteorological conditions," in *Proc. 29th PVSEC Proc.*, Amsterdam, The Netherlands, Sep. 2014, pp. 2303–2309.

[37] G. B. Gaines *et al.*, "Development of an accelerated test design for predicting the service life of the solar array at mead, nebraska," Quarterly Techn. Rep., NASA, USA, Feb. 1979.

[38] L. A. Escobar and W. Q. Meeker, "A review of accelerated test models," *Statist. Sci.*, vol. 21, no. 4, pp. 552–577, Nov. 2006.

[39] R. Laronde, A. Charki, D. Bigaud, and P. Excoffier, "Reliability evaluation of a photovoltaic module using accelerated degradation model," in *Proc. SPIE*, 2011, vol. 8112.

[40] M. Koehl, M. Heck, and S. Wiesmeier, "Modelling of conditions for accelerated lifetime testing of Humidity impact on PV-modules based on monitoring of climatic data," *Solar Energy Mater. Solar Cells*, vol. 99, pp. 282–291, Apr. 2012.

[41] J. Berghold *et al.*, "Potential-induced degradation (PID) and its correlation with experience in the field," *Photovolt. Int.*, vol. 19, pp. 85–92, 2013.

[42] M. Kontges *et al.*, "Review of failures of photovoltaic modules," Report IEA PVPS T13-01:2014, Subtask 3.2, 2014.

[43] P. Hacke *et al.*, "Elucidating PID degradation mechanisms and in-situ dark I-V monitoring for modeling degradation rate in CdTe thin-film modules," *IEEE J. Photovolt.*, vol. 6, no. 6, pp. 1635–1640, Nov. 2016.

[44] P. Hacke *et al.*, "Accelerated testing and modeling of potential-induced degradation as a function of temperature and relative humidity," *IEEE J. Photovolt.*, vol. 5, no. 6, pp. 1549–1553, Nov. 2015.

[45] V. Naumann *et al.*, "Potential-induced degradation at interdigitated back contact solar cells," *Energy Procedia*, vol. 55, pp. 498–503, Jan. 2014.

[46] A. Halm *et al.*, "Potential-induced degradation for encapsulated n-type IBC solar cells with front floating emitter," *Energy Procedia*, vol. 77, pp. 356–363, Aug. 2015.

[47] R. Swanson *et al.*, "The surface polarization effect in high-efficient silicon solar cells," in *Proc. 15th Int. PVSEC Proc.*, Jan. 2005.

[48] D. Lausch *et al.*, "Sodium outdiffusion from stacking faults as root cause for the recovery process of potential-induced degradation (PID)," *Energy Procedia*, vol. 55, pp. 486–493, Jan. 2014.

[49] E. Annigoni *et al.*, "Modeling potential-induced degradation (PID) in crystalline silicon solar cells: From accelerated-aging laboratory testing to outdoor prediction," in *Proc. 32nd EU PVSEC Proc.*, Munich, Germany, Jun. 2016, pp. 1558–1563.

[50] J. Hattendorf *et al.*, "Potential induced degradation in mono-crystalline silicon based modules: An acceleration model," in *Proc. 27th Eur. PVSEC Proc.*, Oct. 2012, pp. 3405–3410.
[51] C. Taubitz, M. Krber, M. Schtze, and M. B. Koentopp, "Potential induced degradation: Model calculations and correlation between laboratory tests and outdoor occurrence," in *Proc. 29th Eur. PVSEC Proc.*, Nov. 2014, pp. 2490–2494.
[52] L. Dunn, M. Gostein, and B. Stueve, "Literature review of the effects of UV exposure on PV modules," in *NREL PV Module Reliab. Workshop*, Feb. 2013.
[53] M. A. Munoz, M. C. Alonso-Garcia, and Vela, "Early degradation of silicon PV modules and guaranty conditions," *Solar Energy*, vol. 85, no. 9, pp. 2264–2274, 2011.
[54] M. Koehl, D. Philipp, N. Lenck, and M. Zundel, "Development and application of a UV light source for PV-module testing," in *Proc. SPIE - Int Soc. for Opt. Eng. 7412*, Aug. 2009, pp. 7412021–7412027.
[55] X. Gu, Y. Lyu, L.-C. Yu, C.-C. Lin, and D. Stanley, "Effect of intensity and wavelength of spectral UV light on discoloration of laminated Glass/EVA/PPE PV module," in *3rd Atlas-NIST Workshop PV Mater. Durability*, Dec. 2015.
[56] D. C. Jordan, T. J. Silverman, J. H. Wohlgemuth, S. R. Kurtz, and K. T. VanSant, "Photovoltaic failure and degradation modes," *Progress Photovoltaics: Res. Appl.*, vol. 25, pp. 318–326, 2017.
[57] N. Bosco, T. J. Silverman, and S. Kurtz, "Climate specific thermomechanical fatigue of flat plate photovoltaic module solder joints," *Microelectron. Rel.*, vol. 62, pp. 124–129, Jul. 2016.
[58] M. D. Kempe, "Evaluation of the uncertainty in accelerated stress testing," in *Proc. IEEE 40th Photovolt. Spec. Conf.*, Jun. 2014, pp. 2170–2175.
[59] A. B. Subramaniyan, R. Pan, J. Kuitche, and G. TamizhMani, "Quantification of environmental effects on PV module degradation: A physics-based data-driven modeling method," *IEEE J. Photovolt.*, vol. 8, no. 5, pp. 1289–1296, Sep. 2018.

Sascha Lindig received the B.Eng. degree in photovoltaic and semiconductor technologies from the University of Applied Science Jena, Jena, Germany, in 2011, and the M.Eng. degree in environmental and energy engineering from the Leipzig University of Applied Sciences, Leipzig, Germany, in 2014. He is currently working toward the Ph.D. degree in electrical engineering with the University of Ljubljana, Ljubljana, Slovenia, in collaboration with EURAC Research, Bolzano, Italy.

He is working in the frame of the Marie Sklodowska Curie SOLAR-TRAIN project on statistical performance loss models of PV systems, degradation patterns and solar economics.

Ismail Kaaya was born in Uganda. He received the B.S. degree in applied physics from the International University of Africa, Khartoum, Sudan, in 2013, the Postgraduate Diploma degree in condensed matter physics from the Abdus-Salam International Center for Theoretical Physics, Trieste, Italy, in 2015, and the M.S. degree in renewable energy science and technology from Ecole Polytechnique, Palaiseau, France, in 2016. He is currently working toward the Ph.D. degree in photovoltaics with Fraunhofer Institute for Solar Energy Systems, Freiburg, Germany.

His research interests includes advanced characterization of hydrogenated amorphous silicon, modeling spatial inhomogenities/(microscopic defects) in solar cells, and development of service life models for PV modules.

David Moser received the B.Sc. and M.Sc. degrees from the University of Trento, Italy, in 2003 and 2006, respectively, the Ph.D. degree in physics from the Salford University, Salford, U.K., in 2010.

He coordinates the activities of the research group Photovoltaic Systems, Institute for Renewable Energy, EURAC, Bolzano, Italy. His work focuses on characterizing indoor and outdoor behavior, performance, and reliability of photovoltaic (PV) modules and systems, building integration of PV systems, and monitoring of outdoor PV plants. He is also active in PV potential studies on a regional scale and member of the Board of Directors of The Association of European Renewable Energy Research Centres.

Karl-Anders Weiß received the Diploma degree in physics and economics and the Ph.D. degree in physics from the University of Ulm, Germany, in 2005 and 2014, respectively.

He is Head of the Service Life Analysis Group, Fraunhofer Institute for Solar Energy Systems, Freiburg, Germany. His areas of interest include degradation of materials in solar applications, accelerated testing of components and materials of solar systems, numerical simulations, methods to analyze degradation of polymers, nondestructive analytical methods climatic loads and service life prediction.

Marko Topic received the Ph.D. degree from the University of Ljublana, Slovenia, in 1996.

He is the Head of Laboratory of Photovoltaics and Optoelectronics, University of Ljubljana, Ljubljana, Slovenia, acts as the Chairman of the European Technology and Innovation Platform Photovoltaics (ETIP-PV) since 2016 and previously as the Chairman of European Photovoltaic Technology Platform (since 2014). He is currently a full Professor with the Faculty of Electrical Engineering at the University of Ljubljana, and he has a very broad research experience in photovoltaics, thin-film semiconductor materials, electron devices, optoelectronics, electronic circuits, and reliability engineering.

Dr. Topic is a member of the Slovenian Academy of Engineering and has received several prestigious awards, including the "Zoisova nagrada" in 2008 (the highest award of the Republic of Slovenia for Scientific and Research Achievements).